

# Unsteady Response of Flow System around Balance Piston in a Rocket Pump

Satoshi Kawasaki\*, Takashi Shimura\*, Masaharu Uchiyumi\*, Mitsuaki Hayashi\*\* and Jun Matsui\*\*\*

\* Japan Aerospace Exploration Agency

1, Koganezawa, Kakuda, Japan

\*\* IHI Corporation

1, Shin-Nakahara-Cho, Isogo-ku, Yokohama, Japan

\*\*\* Yokohama National University

79-5, Tokiwadai, Hodogaya-ku, Yokohama, Japan

## Abstract

In the rocket engine turbopump, a self-balancing type of axial thrust balancing system using a balance piston is often applied. In this study, the balancing system in an LH2 rocket pump was modelled combining the mechanical structure and the flow system, and the unsteady response of the balance piston was investigated. The axial vibration characteristics of the balance piston with large amplitude were determined, sweeping the frequency of the pressure fluctuation on the inlet of the balance piston. This vibration was significantly affected by the compressibility of LH2.

## 1. Introduction

Usually, the rocket engine turbopump must be operated at a very high rotating speed to deliver the high pressure liquid propellant to the combustor. Consequently, large axial thrust is generated on the rotor assembly of the turbopump. Therefore, it is essential to reduce or balance the axial thrust for the reliability of bearings supporting the rotor assembly. The self-balancing type axial thrust balancing system using balance piston is often applied in the rocket engine turbopump. In designing this balancing system, accurate prediction of the axial thrust characteristics is very important.

Figure 1 shows a typical rocket engine turbopump configuration and its internal flow paths. The rotor assembly is allowed to move in the axial direction and shift to the balancing point automatically. However, too much axial vibration not only destroys bearings but also causes metal to metal rubbing which can cause explosion. To avoid these problems, it would be helpful for design of the rocket engine turbopump to simulate the unsteady response of the balancing system and clarify the vibration mechanism.

Kurokawa [1] examined axial thrust behaviour in a rocket pump calculated by steady theoretical analysis of the internal flow. The analysis code developed with this theoretical analysis was applied to investigate the axial thrust characteristics [2], [3]. Della Gatta [4] investigated the axial thrust balance by steady CFD analysis. The obtained results suggest that the methods to predict steady axial thrust can be used in designing turbopump.

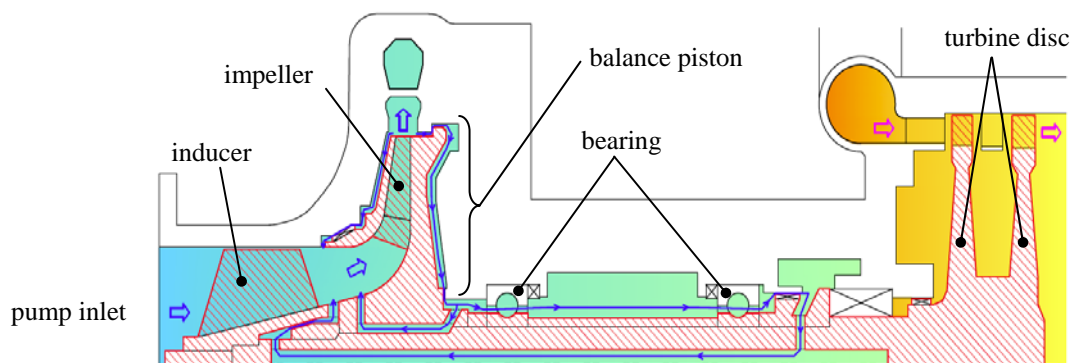


Fig. 1 An example of rocket LH2 pump and internal flow paths

Furthermore, transient axial thrust was calculated during start transient of a rocket turbopump by Hooser [5]. This code was extended to model transient flow to predict time-dependent flow characteristics and good agreement was observed between measurements and predictions.

Dynamic characteristics of the clearance flow have also been investigated. Childs [6] and Brennen [7] have examined the dynamic characteristics of flows in the clearance between the casing and front shroud of impellers by the bulk flow model. By experiments and computations, the dynamic characteristics of the flow between stationary and rotating disks under axial oscillation have been examined by Horiguchi [8]. However, the unsteady response of the balance piston, which is an important device for axial thrust balance, has not been clarified.

In the present study, the balancing system around the balance piston was modelled combining the mechanical structure and the flow system, and the unsteady response of the balance piston was investigated.

## 2. Nomenclature

$f$	[Hz]	frequency of axial vibration
$f_n$	[Hz]	natural frequency
$F$	[N]	axial thrust
$F^*$		normalized axial thrust = $F / (\pi R_{im}^2 \times p_{in})$
$K$	[N/m]	stiffness of balance piston
$M$	[kg]	mass of rotor assembly
$p$	[Pa]	pressure
$p^*$		normalized pressure = $p / p_{in}$
$R_{im}$	[m]	radius of impeller
$S$	[m]	clearance of orifice
$S^*$		normalized clearance of orifice = $S / (S_1 + S_2)$
$T$	[K]	temperature of LH2
Subscripts		
$bp$		balance piston or balance piston chamber
$in$		inlet of balance piston (discharge of impeller)
$oth$		other than balance piston
$1, 2$		inlet orifice (#1) and outlet orifice (#2) of balance piston, respectively

## 3. Balance piston

Figure 2 shows an axial thrust self-balancing system using a balance piston. The balance piston consists of two orifices and a chamber surrounded by these two orifices. The inlet orifice (#1) is located at the impeller outlet and the outlet orifice (#2) is located at the small-radius position of the back shroud. The rotor assembly is allowed to move in the axial direction to control the clearances of the orifices. If unbalance axial thrust is imposed on the rotor assembly in the direction from the pump inlet side toward the turbine part, the rotor assembly moves toward the turbine side. As a result, the clearance of orifice #1 increases and that of orifice #2 decreases. This causes the

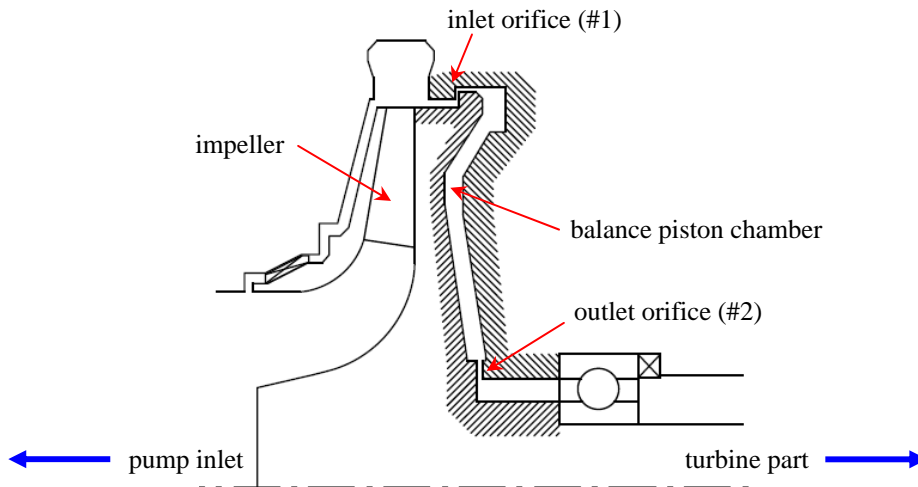


Fig. 2 Configuration of balance piston

pressure in the balance piston chamber to increase, and hence the axial thrust in the direction from the turbine part toward the pump inlet side increases. In this way, unbalance axial thrust imposed on the rotor assembly can be compensated automatically.

In the balance piston chamber, the radial pressure distribution is mainly determined by the centrifugal force effect caused by swirl in the chamber. The axial thrust generated by the balance piston can be calculated by integration of that radial pressure distribution

#### 4. Calculation method

In this study, the axial balancing system was modelled and calculated using a 1D multi-domain system simulation tool, AMESim (Rev.10) [9]. This tool had been previously used for transient modelling and simulation of cryogenic rocket engine [10]. Figure 3 shows the model in which the balancing system of typical LH2 pump [see Fig. 1] is expressed. The model consists of the mechanical structure of the balance piston and the flow path along the back side of the impeller. The balance piston is pushed by the axial thrust generated by the pressure in the balance piston and pulled by that generated in locations other than balance piston. The orifice clearances are connected with displacement of balance piston by the function component (1). The volume of the balance piston chamber is varied with the balance piston displacement. This chamber model is not able to treat pressure distribution inside the chamber, although the balance piston chamber has radial pressure distribution. In this model, the equivalent radial pressure drop estimated by integration of the pressure distribution, which is calculated by steady analysis of the internal flow [3], is given to this chamber model by the function component (2). The downstream path of orifice #2 is expressed by a simple model (chamber, restriction and tank component). In order to investigate the unsteady response of the balancing system, the pressure fluctuation on the inlet of the balance piston was input. The fluctuation frequency was swept from 0 Hz to 2000 Hz and the fluctuation amplitude was 10% of the inlet pressure of the balance piston. Other calculating conditions are described as follows:

- Thermal fluid properties of LH2 was given by polynomials approximation.
- Total clearance of orifice #1 and orifice #2 is axially about 0.3 mm.
- Rotating speed was 50000 rpm.  
 (Rotating speed was not used in this-code directly, but was used in the steady analysis code.)
- Temperature in the inlet of the balance piston was 28 K unless otherwise indicated.
- Heat caused by disk friction of the impeller was not considered.
- Heat input from outside of turbopump was not considered.
- Cavitation was not considered.
- Damping caused by the balancing system was not considered.

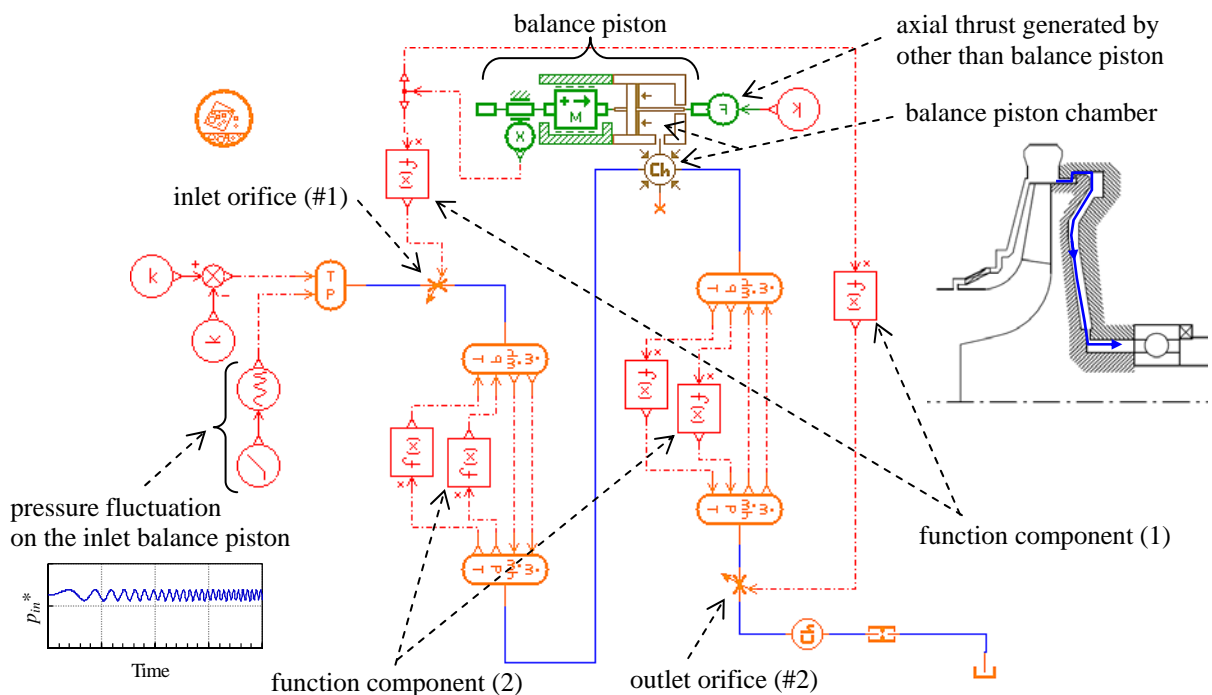


Fig. 3 Model structure of internal flow system around balance piston

### 5. Results

First of all, to verify that the present model could achieve balance at proper positions, steady state calculation by this model was carried out and compared with the results of the steady analysis of the internal flow [3]. Figure 4 shows static axial thrust characteristics of balance piston. The horizontal axis shows the normalized clearance of orifice #1 and the vertical axis shows the axial thrust generated by the balance piston. The positive direction of thrust was from the turbine part to the pump inlet side. The result of the present code showed good agreement with that of the steady analysis code. The equivalent pressure in the balance piston chamber was given by the result of the steady analysis code. The small difference between the results of the present code and that of the steady analysis was caused by accuracy of the equivalent radial pressure drop estimation. It was confirmed that the present balancing system model could estimate the axial balancing position in steady state. The slope of these curves means the static stiffness (spring rate) of the balance piston brought by the fluid force change due to the piston displacement, which depends on the relationship between the pressure drop of orifice #1 and orifice #2. Without damping, the natural frequency of the balance piston is expressed as follows:

$$f_n = \frac{1}{2\pi} \sqrt{K/M} \tag{1}$$

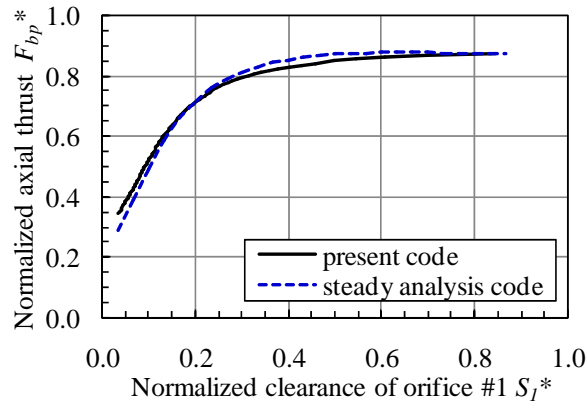


Fig. 4 Static axial thrust curves of balance piston

By inputting the pressure fluctuation on the inlet of the sweeping frequency of the balance piston, the unsteady response of the balance piston was calculated by the present model. Figure 5(1) shows the clearance of orifice #1 and the pressure of the balance piston chamber to show the behaviour of the balance piston. Figure 5(2) shows FFT results of these data. The large amplitude vibration of the balance piston and the pressure fluctuation in the chamber were determined at about 1200 Hz. The mean normalized clearance of orifice #1 was about 0.27 and the natural frequency of the balance piston was 900 Hz which was calculated by the static axial thrust characteristics of the balance piston and Eq.(1). There is a slight difference of the vibration frequency with large amplitude.

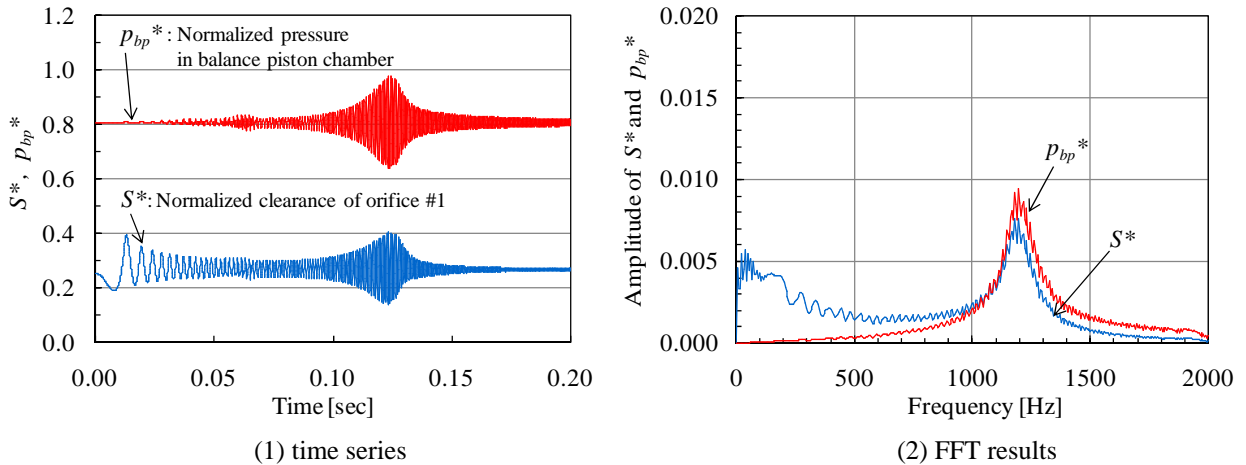


Fig. 5 Calculation results with base condition

In order to investigate the effects of the static stiffness of the balance piston, the axial thrust generated in the locations other than the balance piston,  $F_{oth}$ , was decreased. With the reduction of  $F_{oth}$ , the static balancing point was moved toward the pump inlet side. The calculation result is shown in Fig. 6. According to the static axial thrust characteristics of the balance piston [see Fig. 1], the stiffness of the balance piston is expected to be larger and the natural frequency is expected to be higher when the orifice #1 clearance is decreased. In the results shown in Fig. 5 and Fig. 6, the mean normalized orifice #1 clearance became 0.26 and 0.2 and the natural frequency calculated by the characteristic curve of the static axial thrust became 900 Hz and 1200 Hz respectively. However, the peak vibration frequencies of the two results shown in Fig. 5 and Fig. 6 were not so different (about 1200 Hz). This means that these vibrations were not determined by only the static stiffness slope of the curve, but were affected by other factors.

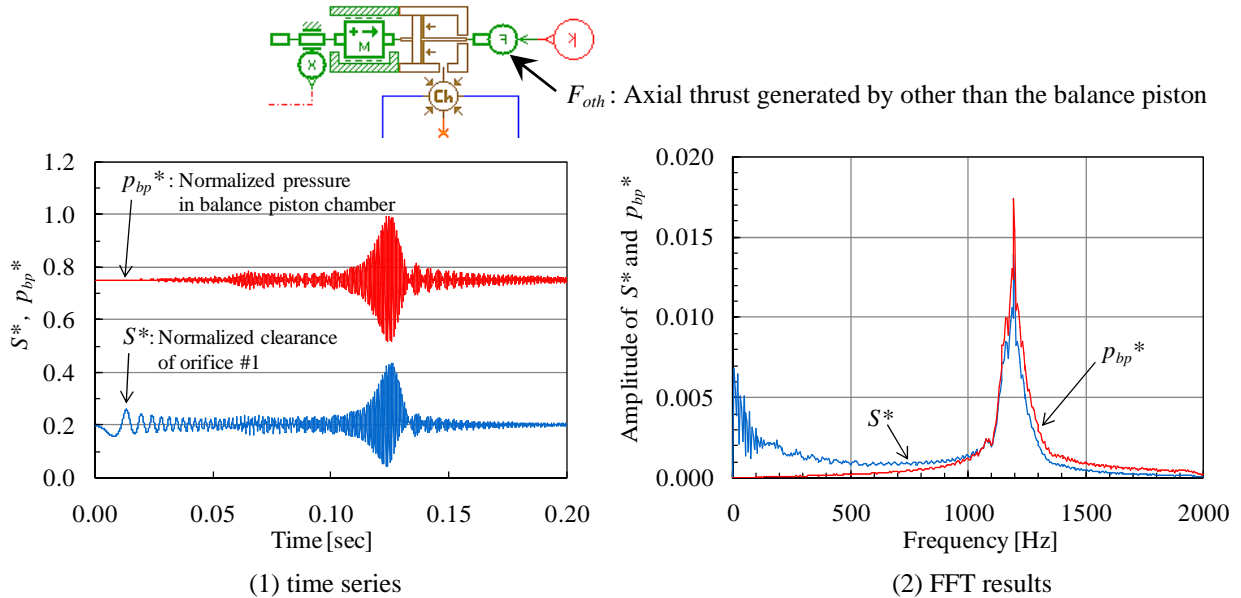


Fig. 6 Calculation results with 7%  $F_{oth}$  less than that of the base condition

As another factor, the compressibility of LH2 is conceivable, because the bulk modulus of LH2 is considerably smaller than that of a typical liquid. As the bulk modulus of LH2 is quite variable depending on the temperature, the calculation was carried out by the condition at a temperature different from that of base condition, The calculation result is shown in Fig. 7, when the temperature on the inlet of the balance piston,  $T_{in}$ , decreased to 24 K. The axial vibration with large amplitude was determined at about 1400 Hz which was 200 Hz higher than that of the base condition. The bulk modulus of LH2 at a temperature of 24 K is 1.38 times larger than that at a temperature of 28 K. The natural frequency of the liquid is proportional to the square root of the bulk modulus, so that the natural frequency of LH2 at the temperature of 24 K is 1.2 times higher than that at the temperature of 28 K. The peak vibration frequency of the case at  $T_{in}=24$  K is 1.2 times higher than that at  $T_{in}=28$  K. This means that the large vibration of the balance piston was significantly affected by the compressibility of LH2.

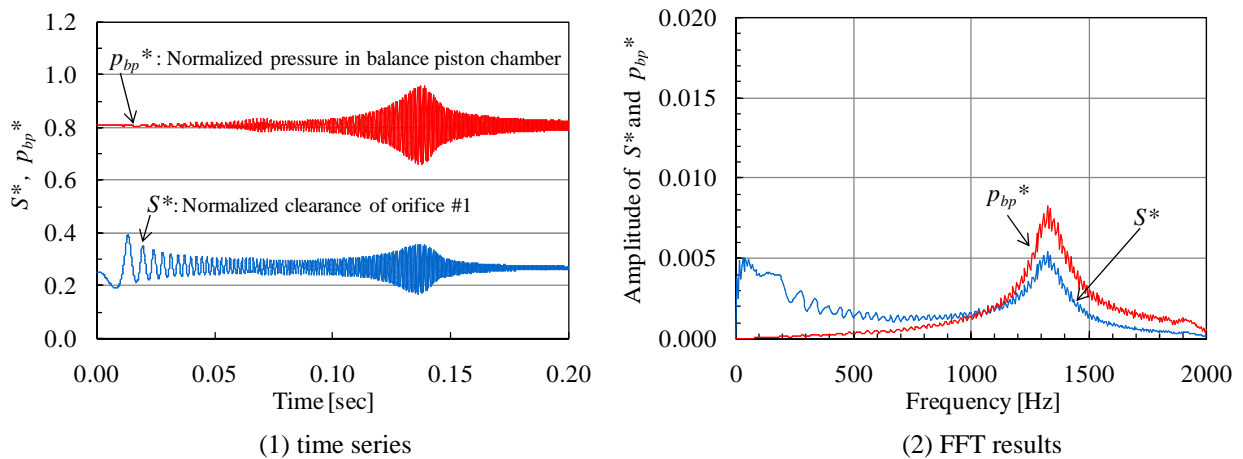


Fig. 7 Calculation results with 4 K  $T_{in}$  lower than that of the base condition

If the balance piston chamber volume increases, the stiffness of the liquid in the balance piston decreases. Figure 8 shows the calculation results when volume of the balance piston chamber,  $V_{bp}$ , was 50% larger than that of the base condition by extending the chamber clearance. The axial vibration with large amplitude was determined at about 1000 Hz, which was 200 Hz lower than that of the base condition, and the peak amplitude of the vibration was about twice that of the base condition. The characteristic curve of the static axial thrust of this case was the same as that of the base condition as shown in Fig.5 and Fig. 9. This means that the difference between these large vibrations was not due to the static axial thrust characteristics but rather due to the compressibility of LH2.

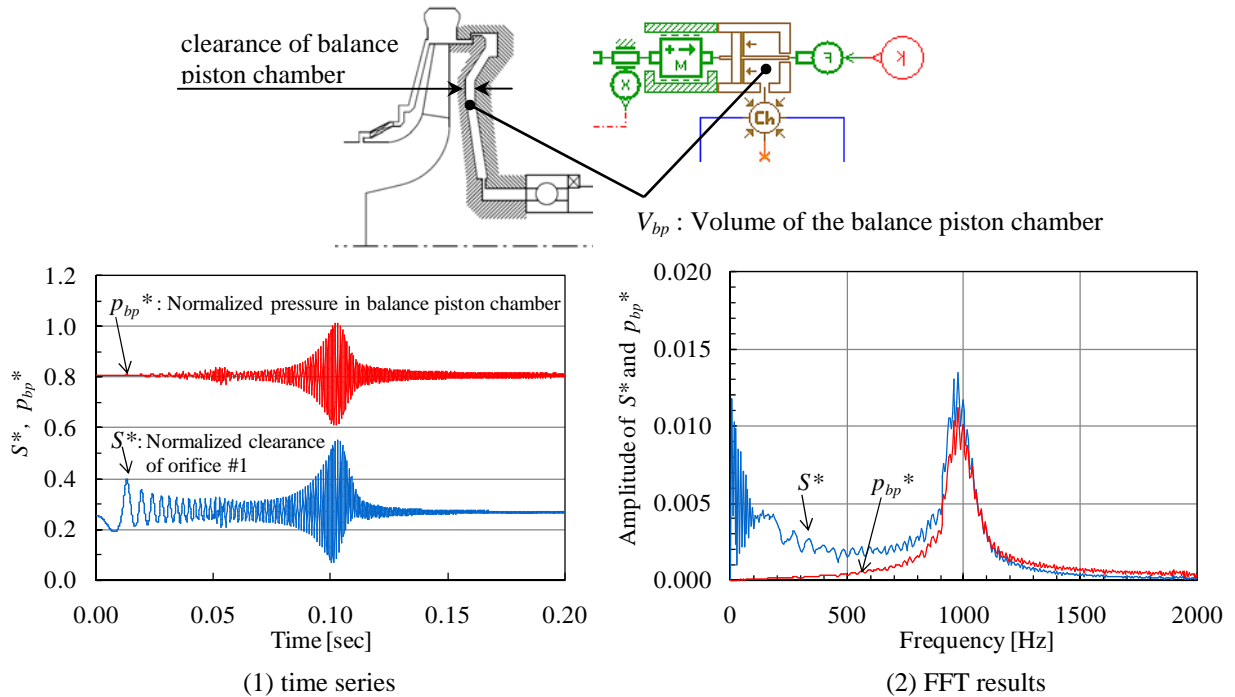


Fig. 8 Calculation results with 50%  $V_{bp}$  larger than that of the base condition

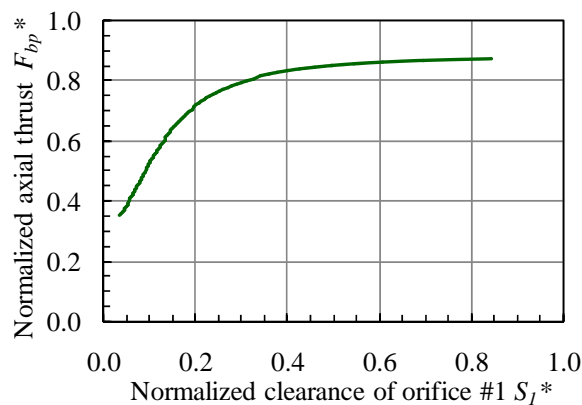


Fig. 9 Static axial thrust curve of balance piston with 50%  $V_{bp}$  larger than that of the base condition

When the volume of the balance piston chamber is larger, the amplitude of the axial vibration due to the liquid compressibility is larger. To restrain the axial vibration, the balance piston chamber volume should be as low as possible for the high compressible liquid in designing the balance piston. Developing that idea, there is some possibility to control the axial vibration using the liquid compressibility like as an accumulator. For that purpose, it is necessary to develop a more accurate model.

Finally, the calculation time of each case is about 10 seconds by a typical personal computer.

## 6. Conclusions

The internal flow system around the balance piston in an LH2 rocket pump was modelled and the unsteady response of balance piston was investigated, inputting the pressure fluctuation on the inlet of the balance piston.

- (1) The balancing system could be modelled combining the mechanical structure and the flow system.
- (2) Sweeping the frequency of the pressure fluctuation on the inlet of the balance piston, the axial vibration of the balance piston with large amplitude was determined.
- (3) This large vibration was significantly affected by the compressibility of LH2. Therefore, the vibration is influenced by the bulk modulus of LH2 and the volume of the balance piston chamber.
- (4) This unsteady code is able to estimate the axial vibration frequency of the balance piston taking account of the effect of the liquid compressibility.

## References

- [1] Kurokawa, J., Kamijo, K. and Shimura, T., 1994, Axial Thrust Behavior in LOX-Pump of Rocket Engine, *J. Propulsion and Power*, Vol. 10, No. 2, 244-250.
- [2] Abe, H., Matsumoto, K., Kurokawa, J., Matsui, J. and Choi, Y., 2006, Analysis and Control of Axial Thrust in Centrifugal Pump by Use of J-Groove, *23rd IAHR Symposium-Yokohama*.
- [3] Shimura, T., Kawasaki, S., Uchiumi, M. and Matsui, J., 2011, Internal Flow and Axial Thrust Balancing of a Rocket Pump, *Proc. ASME-JSME-KSME Joint Fluids Engineering Conference 2011*, AJK2011-06027, Hamamatsu, Japan. (to appear in)
- [4] Della Gatta, S., Sslvadori, S., Adami, P. and Bertolazzi, L., 2006, CFD Study for Assessment of Axial Thrust Balance in Centrifugal Multistage Pumps, *Proc. Conference on Modelling Fluid Flow(CMFF'06), The 13th International Conference on Fluid Flow Technologies*, Budapest, Hungary.
- [5] Hooser, K. V., Bailey, J. and Majumda, A., 1999, Numerical Prediction of Transient Axial Thrust and Internal Flows in a Rocket Engine Turbopump, *35th AIAA/ASME/SAE/ASEE Joint Propulsion Conference*, AIAA-99-2189, Los Angeles, CA.
- [6] Childs, D. W., 1991, Fluid-Structure Interaction Forces at Pump-Impeller-Shroud Surfaces for Axial Vibration Analysis, *Trans. ASME, J. Vibration and Acoustics*, Vol. 113, 108-115.
- [7] Hsu, Y. and Brennen, C. E., 2002, Fluid Flow Equations for Rotordynamic Flows in Seals and Leakage Paths, *Trans. ASME, J. Fluids Eng.*, Vol. 24, No. 1, 176-181.
- [8] Horiguchi, H., Ueno, Y., Takahashi, K., Miyagawa, K. and Tsujimoto, Y., 2009, Dynamic Characteristics of the Radial Clearance Flow between Axially Oscillating Rotational Disk and Stationary Disk, *Int. J. Fluid Machinery and Systems*, Vol. 2, No. 2, 147-155.
- [9] <http://www.lmsintl.com/> (2011).
- [10] Rhoté-Vaney, R., Thomas, V. and Lekeux, A., 2002, Transient Modelling of Cryogenic Rocket Engines: a Modular Approach, *4th International Conference on Launcher Technology Space Launcher Liquid Propulsion*, Liège, Belgium.